2024 IEEE/RSJ International Conference on Intelligent Robots and Systems (IROS)
October 14-18, 2024. Abu Dhabi, UAE

3D Localization of Objects Buried within Granular Material Using a Distributed 3-Axis Tactile Sensor

Zhengqi Chen[1], Elisabetta Versace[2], and Lorenzo Jamone[1]

***Abstract*— While visual sensing is often the predominant modality for a robot to localize objects in the environment, tactile and force sensing become crucial when objects are occluded, poorly visible, or buried. However, existing works on locating buried objects rely solely on force measurements at a single contact point on the robot end-effector, making 3D localization very challenging. This paper presents an alternative approach using a tactile sensor that measures both normal and shear forces (i.e. 3-axis) on distributed points; three Long Short-Term Memory (LSTM) models are trained with real-world data to perform real-time 3D localization (i.e. distance, direction and depth) of an object buried within a granular material. Our experimental results suggest that measuring both normal and shear forces (instead of just normal) on distributed contact points (instead of only one point) is essential for the accurate 3D localization of buried objects.**

I. INTRODUCTION

Vision and touch are two complementary sensory modalities that play crucial roles in human perception and interaction with the external environment [1]. While vision can provide a global image of the surroundings, tactile feedback is confined to the points of contact, presenting information in a sparse form in the absence of exploration strategies. However, when environmental lighting conditions are insufficient to support visual signal acquisition or when the target object is occluded, tactile signals, gathered through physical contact, become more reliable. Tactile signals collected through different forms of contact such as pressing or sliding can be used to perceive and recognise the material (texture, stiffness) and shape of objects [2].

This study draws inspiration from the foraging behavior of birds, which utilize tactile sensory organs on their beaks to perceive the location of buried food items in soil [3]. This presents a challenge for robots: can tactile sensors be relied upon to locate the three-dimensional position of buried objects? Granular materials such as sand, grains, and snow undergo a jamming transition process when subjected to external forces, during which the particles shift from a fluid-like state to a solid-like state [4]. A similar task arises when an end effector rakes into a granular environment and approaches the buried object; only particles within a certain area in front of the end effector, termed the failure zone [5], will move. As the buried object enters the failure zone, the compression of intermediate particles by the object and the end effector pushes them into the jamming state. Detection of the manifestation of the jamming state in tactile sensing marks the onset of estimating the object position [6]. Recently, there has been increasing attention on tasks involving interactions between robots and granular materials [6]–[11]. However, research on the expression of granular material effects in tactile sensing and its application in buried object localization is still limited, necessitating the use of more sensitive sensors with various configurations.

[1]Zhengqi Chen and Lorenzo Jamone are with ARQ (Advanced Robotics at Queen Mary), School of Engineering and Materials Science, Queen Mary University of London, UK `[zhengqi.chen, l.jamone]@qmul.ac.uk`

[2]Elisabetta Versace with the Department of Biological and Experimental Psychology, Queen Mary University of London, UK `e.versace@qmul.ac.uk`

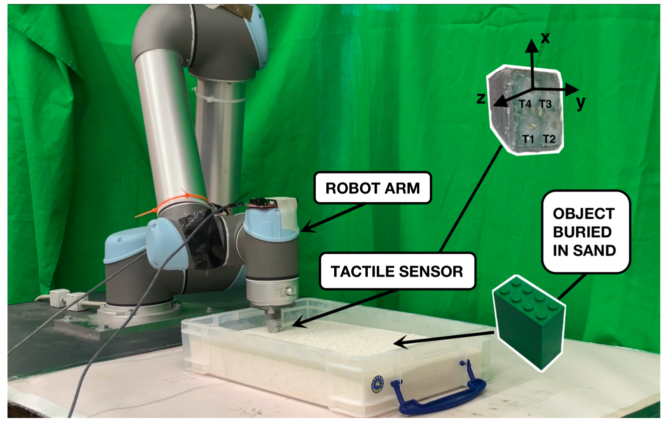

Fig. 1. A UR5 robot equipped with a custom-made 3-axis tactile sensor. The target object under localization is fixed on the bottom of the sand box, rendering it invisible to direct observation.

In this study, we use a three-axis magnetic tactile sensor inspired by the design presented in [12], [13]. Our sensor has four taxels symmetrically distributed around the center, with each taxel capable of detecting shear forces (x- and y-directions) as well as normal forces (z-direction); the sensor is described in more details in [14]. Previous work on buried object detection focused solely on measuring changes in normal force [6], [8]; however, through experimentation, we discovered more pronounced changes in shear forces as the sensor approaches the buried object. Moreover, it is noticed that leveraging the symmetry of horizontal shear forces (y-direction) among different taxels enables spatial localization of the buried object. In inferring object position based on the jamming effect, object position can be determined by the position of the end effector at the time of jamming occurrence and the radius of the failure zone. However, the size of the failure zone directly correlates with parameters such as raking depth, the contact area of the end effector, and the properties of the granular material [6], [15]. To avoid the need of prior information regarding the properties of granular

979-8-3503-7769-9/24/$31.00 ©2024 IEEE

materials, which can be challenging to obtain directly, our work proposes a learning-based model comprising three Long Short-Term Memory (LSTM) models trained on the specific scenario. By reducing the length of input signals to ensure the correctness of training labels and slicing collected tactile data using a sliding window approach as model input, we achieve real-time prediction of the 3D position (distance, direction and depth relative to the current sensor position) of the target object.

To summarize, our key contributions are:

- A novel learning-based model that enables real-time prediction of the distance, direction and depth of buried objects using a tactile sensor;
- Experimental results that demonstrate that both the presence of multiple taxels and the ability to measure shear forces are necessary to accurately detect buried objects with tactile sensors;
- Publicly available code and dataset[1] to replicate our experiments and to extend our results.

II. RELATED WORK

A. Pretouch and tactile sensing

The predictive capability of estimating object position prior to physical contact, akin to the jamming detection method described earlier, is referred to as Pretouch within the domain of tactile sensing. Pretouch serves as a modality positioned between tactile sensing and vision, enhancing tactile perception by extending detection range [16]. In scenarios where camera systems encounter occlusions or are affected by lighting conditions, pretouch perception can respond more effectively to unforeseen events compared to traditional tactile perception, which may necessitate limiting the velocity of the robot to avoid collisions, thereby sacrificing time efficiency [17]. In addition, the application of pretouch helps avoid wear caused by direct contact between sensors and objects, thereby contributing to extending the sensor lifespan. Common pretouch methods encompass sound [18], optical [19] and capacitive measurements. In [20], a pretouch system employing magnetic and capacitive sensors is proposed, capable of predicting the positions of both dielectric and ferromagnetic objects. Similarly, the work presented in [21] utilizes a 3-axis Hall effect sensor to measure position changes induced by an electromagnet. However, existing research on pretouch predominantly focuses on perception in open-air environments, leaving room for investigation into its application in granular materials.

B. Tactile interaction with granular material

The mechanical vibration resulting from the movement of granular particles contains haptic information regarding the properties of objects [22], [23]. Togzhan et al. [10] collect vibro-tactile signals as input to detect the presence of foreign bodies, achieving an accuracy of 91%. In [9], the Digger Finger is designed with a wedge shape to facilitate vertical penetration. Utilizing mechanical vibration, this finger is employed to discern buried objects with varying outlines. As the end effector continuously rakes, the interaction effect from the buried object acts on the sensing surface through force chains [24]–[26], triggering jamming before physical contact with the object occurs. [7] proposes an architecture to integrate three tactile modalities (vibration, internal fluid pressure, and fingerpad deformation) into an input layer of a recurrent neural network (RNN). It is observed that fingerpad deformation provides the most significant evidence for distinguishing between two contact states: free exploration and contact with an object within granular media. Building upon this work, [6] describes another contact state - Jamming, during which a noticeable increase in fingertip force can be observed. An estimated sensor model is developed based on a triaxial shear test, assuming the size of the failure zone ahead of the sensor remains constant. The proposed framework is validated through both simulation and real robot experiments, successfully implementing simultaneous localization and mapping (SLAM) within granular media. [8] presents a granular-material-embedded autonomous proximity sensing system (GRAINS) that localizes buried objects and outlines their distribution. In their latest work [11], a multimodal autoencoder using visuo-tactile signals was proposed to estimate the property of granular materials. However, the above work solely considers the drag force applied on the tactile sensor while overlooking the interaction effect of granular material in shear directions. Furthermore, all the studies have been conducted in a 2D environment without considering depth as a parameter.

III. METHODS

A. Robotic system

The custom-made tactile sensor [14] comprises four taxels with each configured into a 3D vector, as shown in Fig.1, facilitating 12 measurements per time step. When subjected to external force, the displacement of magnet within the silicone layer results in alterations to the magnetic field measured by the Hall effect sensor (MLX90393 magnetic sensor) positioned beneath it. The dimensions of the sensor are 20×23mm, affixed onto a 3D-print fingertip to facilitate penetration. This tactile sensing fingertip is mounted on a UR5 robot and transmits data at a frequency of 15Hz.

The experimental setup involves the utilization of dry sand with grain size ranging from 1-1.5mm to construct the granular environment. The sand is contained within a sandbox of 348×220mm with a depth of 68mm. To simplify the motion of buried objects during exploration by the end effector, object is fixed throughout the entirety of the experiments. Lego components with 16×32mm dimensions and varying heights are fixed onto a Lego plate positioned at the bottom of the sandbox.

B. Prediction model

At the outset of the experiment, the tactile sensor undergoes calibration and zero-set procedures to ensure that its measurements solely respond to external forces applied to it.

[1] `https://github.com/ERICHEN25/Tactile-3DLocalization`

Upon the fingertip reaching the start position within the sand, ROS nodes responsible for recording tactile measurements and fingertip coordinates commence operation and transmit data to the prediction model.

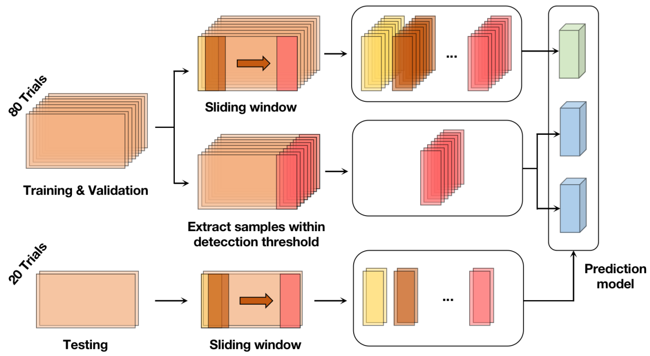

Fig. 2. Pipeline for Prediction Model Construction. The normalized tactile feedback from training and validation datasets were processed independently to feed into the prediction model (distance regressor is depicted in green while direction and depth classifiers are depicted in blue). Subsequently, the trained prediction model underwent evaluation using sliding windows partitioned from the testing dataset.

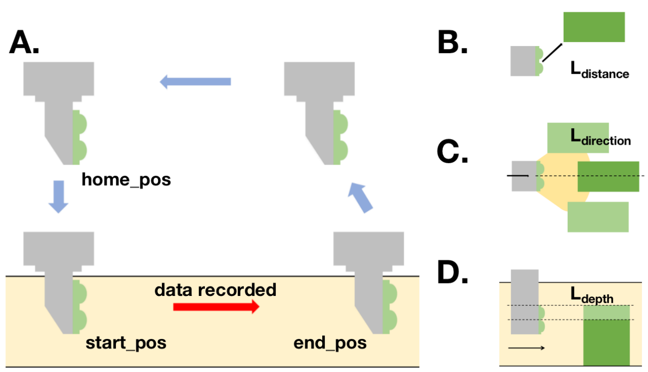

Fig. 3. The trajectory of the experiments is illustrated in (**A**), The trajectory that tactile measurements and Cartesian coordinates of the sensor were recorded is illustrated in red. Our experiments were designed based on three prediction labels: (**B**) Shortest distance between the sensor center and the object outline. (**C**) Object is localized either on the left/right of the object or centered in front. (**D**) Two depths of object buried in.

Instead of training a singular model to directly predict the 3D object position, we developed three distinct Long Short-Term Memory (LSTM) models independently. Each model is tasked with estimating a specific parameter: distance, direction (classifier), and depth (regressor) of the buried object at the current time step. When utilizing tactile data for jamming detection, tactile measurements exhibit temporal dependencies, where the value at a certain time step depends on the values at previous time steps. LSTMs excel at modeling such sequential dependencies by processing the input data sequentially through time steps while retaining memory of past observations. Our preliminary experiments have revealed that the initiation of detection for various parameters does not occur simultaneously. Therefore, this division into three models not only simplifies the complexity of model learning but also enables a more comprehensive evaluation of each parameter individually. When functioning as a unified prediction model, the estimated object position relies predominantly on the output of the distance model when the object is distant. When the distance model predicts that the object is in proximity, the predictions from the direction and depth models are integrated to facilitate 3D localization.

Distance model: A regressor that trained on all the clipped windows of the tactile data.

Direction model: A classifier that trained on the samples collected when the object is within the detection threshold, as determined by the distance prediction (discussed in Section V), accompanied by 3 direction labels.

Depth model: A classifier that trained on the samples collected when the object is within the same detection threshold, accompanied by 2 depth labels.

In Section V we introduce the raking experiments and data collection process. Moreover, we further elucidate the structure of the three models and corresponding training procedures.

IV. EXPERIMENT DESIGN

As the tactile sensor approaches the buried object, detection of the object only occurs when it enters the failure zone of the sensor. However, modeling the failure zone proves infeasible without measuring the sand properties, posing challenge to the labeling of collected samples (i.e. labels for direction and depth of the buried object). Consequently, we truncated the samples to retain only the final segment where object detection is assured. We employed a sliding window technique to partition the lengthy sequences into smaller windows, which then served as input for the direction and depth models. For the distance model, we applied the same sliding window technique across the entire tactile sequence to derive the inputs. The trained LSTM models, specifically tailored for processing these shorter sequences, were then evaluated on the testing dataset. Fig. 2 shows the pipeline of building the prediction model.

A. Data Collection

To represent the 3D localization of an object, three parameters are essential for this study: the distance between the buried object and the sensor, the direction of the object towards the sensor and the buried depth of the object at the current time step. Cubic objects of two different heights are positioned at varying locations relative to the tactile sensor for each trial of the moving trajectories. As illustrated in Fig. 3, every trajectory of the end effector begins from the home position in mid-air, descends into the sand until reaching the start position at a depth of 30mm. The end effector maintains a consistent speed of 20mm/s along a straight-line trajectory during raking. Once it reaches the end position, movement halts, followed by a return to the home position. Through preliminary experimentation, an approximate failure zone was determined for the current setup. Subsequently, objects in all experimental trials are positioned within this area to ensure jamming detection during raking while maintaining a safe distance (over 10 mm) from the end position. From the top view, objects are positioned at various distances away from the end position, with a horizontal distance (along the raking direction) ranging from 10 to 15 mm and a vertical distance ranging from 0 to 15 mm. Tactile measurements and Cartesian coordinates of the sensor were recorded from the start position to the end position. At every time step t, the output of the prediction model updates three labels $L_t = \{L_{1,t}, L_{2,t}, L_{3,t}\}$ representing the object location. The distance label L_1 is calculated as the shortest distance from the center of the sensor to the object, utilizing real-time Cartesian coordinates of the sensor in conjunction with the known position of the fixed object. The direction label L_2 indicates three directions relative to the sensor, with 0, 1 and 2 corresponding respectively to "on the left", "centered in front" and "on the right". The depth of the buried object is denoted by L_3, where a value of 0 for "the same height as the sensor" and a value of 1 for "half the height of the sensor". Raking trials were conducted with varied object locations, yielding a total of 100 trials sampled at a rate of 15 Hz. Of these, 60 trials were allocated to the training dataset, while the 20 trials were designated as a validation dataset and remaining 20 trials for a testing dataset.

B. 3D Localization Model

The acquired tactile data undergoes min-max normalization that applied to each feature B_i where $i \in (1, 12)$, resulting in normalized features $B_i^{'}$ within the range of (0, 1).

$$B_i^{'} = \frac{B_i - B_{\min,i}}{B_{\max,i} - B_{\min,i}} \tag{1}$$

The normalized tactile data were then segmented into multiple windows. To prevent learning order-specific bias and temporal dependencies in training, the windows were shuffled before being fed into the LSTM. Each of the window consists of 5 (time steps) × 12 (features) resulting in 60 tactile measurements for each input.

Distance model: The distance model works as a regressor that estimate the shortest distance between the sensor center and the object surface at each time step. Therefore, normalized dataset were sliced to fit a window size of 5 and a stride of 1 time step (i.e. 1-5 steps, 2-6 step...). The tactile features are processed as follow:

$$y = f(W_{out} h_T + b_{out}) \tag{2}$$

where W_{out} and b_{out} are the weight matrix and bias vector of the output layer, respectively, and f is the activation function (i.e. linear) for regression. The final hidden state h_T is used as input to the output layer after processing all 5 time steps. Adam optimization algorithm is utilized as the optimizer, with mean-squared error serving as the loss function. The LSTM model contains 2 hidden layers with 100 and 50 units respectively and was trained for 400 epochs with a batch size of 128.

Direction model: The direction model comprises 2 hidden layers featuring 100 and 200 neurons and an output layer with 3 units corresponding to direction labels (i.e. "on the left," "centered in front," and "on the right"). Softmax was used as the activation function to obtain probabilities over the output classes. Rmsprop is used as the optimizer, with cross-entropy serving as the loss function for the 3-class classification task, encompassing labels 0, 1, or 2. The direction models are trained for up to 400 epochs with a batch size of 32.

Depth model: The input of the depth model is the same as that of the direction model. Featuring the the same structure as the direction model and an output layer responsible for classifying data into 2 depth labels, the model underwent training for 200 epochs, utilizing a minibatch size of 64.

In this study, our focus lies in investigating whether incorporating shear forces enhances predictive accuracy when compared to utilizing normal force alone. Additionally, we aim to assess whether employing a symmetrical taxel array yields better performance compared to utilizing a single taxel. To achieve this objective, we selected four distinct types of inputs for validation purposes: solely normal force on a single taxel (z_1), three-axis forces on a single taxel (x_1, y_1 and z_1), normal force on four taxels (z_1, z_2, z_3 and z_4), and three-axis forces on four taxels (all 12 features). Consequently, four prediction models were developed, each corresponding to a specific type of input. It is noteworthy that only the size of the input layer was adjusted to accommodate the respective input data size; the training setup remained consistent across all models.

V. RESULTS

In this section, we present the primary outcomes derived from the comparison of various tactile inputs. In summary, our experimental results confirm the hypothesis that distributed 3-axis tactile sensing facilitates 3D localization. Furthermore, we observed that incorporating shear forces as model inputs significantly improves prediction accuracy in comparison to relying solely on normal force. Below, we provide additional insights into these findings.

A. Evaluation of Distance Prediction

The performance of the distance prediction models was evaluated by comparing the predicted distances with the actual distances over the entire trajectory, as illustrated in Fig. 4. The ground truth, indicated by the red dashed line, serves as the reference for actual distances to the object. Our analysis reveals that while model predictions generally follow the ground truth trend, notable deviations occur, particularly when the sensor is more than 45 mm away from the object, where all models consistently overestimate distances by approximately 60 mm. The divergence between predicted and actual distances in this range is attributed to the variation in the starting points of the training and testing datasets—170 mm and 110 mm from the object, respectively. Despite similar initial tactile data readings in both datasets, models trained on training dataset tend to reflect distance labels learned during training rather than adapting to the closer actual distances encountered in testing

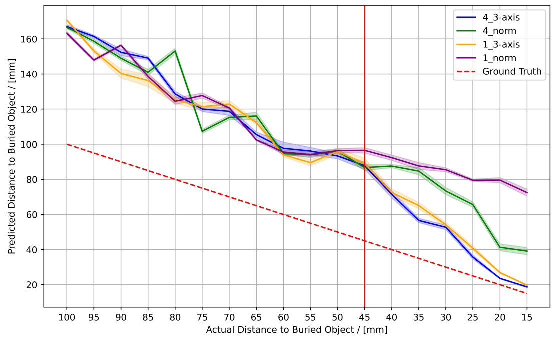

Fig. 4. Distance prediction for models with four types of inputs. The actual distance, serving as the ground truth, is represented by a red dashed line. Models trained with 3-axis forces demonstrate decreasing prediction error as the object's distance falls below 45 mm (detection threshold), indicated by the red solid line.

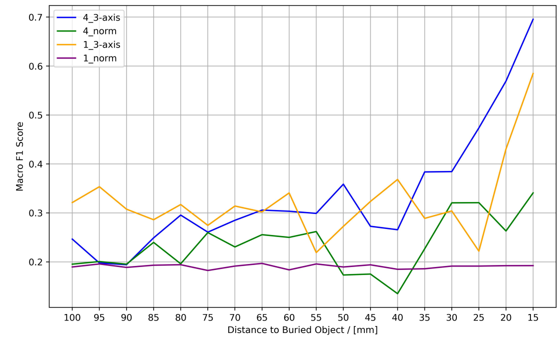

Fig. 5. Macro F1 scores for the direction models with 4 types of inputs. Using 3-axis forces as the model inputs resulted in better performance compared to the normal-only force models.

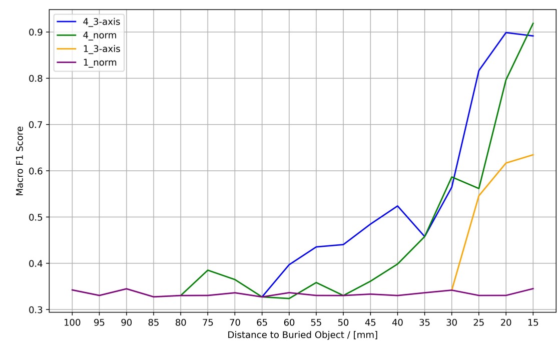

Fig. 6. Macro F1 scores for the depth models with 4 types of inputs. Using tactile data from four taxels as the model inputs achieved higher prediction accuracy.

scenarios. This observation underscores the flexibility of our methodology to accommodate trajectories of varying lengths, provided the jamming process is accounted for. The divergence in model predictions varies with trajectory length, yet consistently, the detection threshold can be effectively identified by pinpointing the onset of a marked reduction in divergence. As sensors approach within 45 mm of the object, models utilizing three-axis forces as inputs (depicted in blue and orange in Fig. 4) produce more and more accurate predictions as the object is closer. This observation confirms our preliminary findings that shear forces, unlike normal forces, are sensitive to the jamming effects caused by proximity to the buried object. The 45 mm mark emerges as a critical detection threshold where model accuracy significantly improves, aligning with the "failure zone" theory in granular interaction. This threshold is consequently adopted for truncating samples in subsequent directional and depth prediction tasks, highlighting the importance of incorporating multi-axis tactile data to enhance prediction reliability and accuracy in proximity detection applications.

B. Evaluation of Direction Prediction

The evaluation results of the direction classifiers are illustrated in Figure 5. Macro F1 scores of all the N samples for the i-th distance class were computed to assess model performance across varying distances to the buried object.

$$\text{Macro F1} = \frac{1}{N}\sum_{i=1}^{N}\frac{2\cdot \text{Precision}_i\cdot \text{Recall}_i}{\text{Precision}_i+\text{Recall}_i} \tag{3}$$

The single normal force model maintains consistently low performance throughout the range, with a macro F1 score stabilizing around 0.2, showing minimal improvement even as the object comes closer. This suggests that relying solely on a single normal force is insufficient for accurate object detection at various depths. In contrast, models incorporating shear forces demonstrate more variability but improved performance as the object gets closer. The single 3-axis model shows best at longer distances and experiences a sharp rise in F1 score as the object approaches 25 mm, peaking at around 0.57. The four 3-axis model follows a more stable trajectory, steadily improving from 40 mm onward and reaching a maximum F1 score of 0.7 at 15 mm. This highlights the effectiveness of shear force data, especially when used in combination with multi-axis measurements, for enhanced detection sensitivity in closer ranges. The model that incorporates normal forces from four taxels, while demonstrating relatively stable performance, shows a minor improvement compared to the 3-axis models. This suggests that while the use of multiple taxels enhances stability, it is less effective at detecting objects at specific directions compared to models utilizing shear forces.

C. Evaluation of Depth Prediction

Assessed using the same metric, the prediction outcomes of the depth models are depicted in Figure 6. Models that incorporate both normal and shear forces from four taxels demonstrate a clear performance advantage, achieving the highest F1 score across nearly the entire trajectory. This aligns with the result of direction prediction. In contrast, the 4-normal-force model exhibits a significant improvement in performance as approaching the buried object, reaching a peak F1 score close to 0.9 at the shortest distance (15 mm). This contrasts sharply with its behavior in Figure 5, where it shows more modest performance and exhibited greater fluctuation across distances. This difference highlights the distinct sensing requirements for depth versus direction, where depth estimation benefits more from spatially distributed normal forces, whereas direction requires a combination of both shear and normal forces for higher accuracy.

VI. CONCLUSIONS

In this work, we achieved 3D localization of buried object using a distributed 3-axis tactile sensor. Our learning-based approach relies on three LSTM models, to predict the distance, direction, and depth of the buried object, respectively. By categorizing inputs based on whether they originate from a symmetrical tactile array and the presence of induced shear forces, we conducted evaluations across these three scales. Our results demonstrates that both the presence of multiple taxels and the ability to measure shear forces are essential factors for accurately localizing buried objects within a 3D space. In addition, it points out the shear forces led by the jamming effect are more crucial than the normal force in 3D localization.

To the best of our knowledge, this represents the first instance of showcasing 3D localization for a object buried within granular material using tactile sensing exclusively. We anticipate that our findings will stimulate greater interest in tactile interaction with granular materials and its potential applications in robotics, particularly concerning buried object localization. In the future, we envision extending this work by developing more robust prediction frameworks and seamlessly integrating them into real-world robotic applications.

ACKNOWLEDGMENT

The authors would like to thank the China Scholarship Council for financial support for this research through the certification No. 202208060081.

REFERENCES

[1] N. Navarro-Guerrero, S. Toprak, J. Josifovski, and L. Jamone, "Visuo-haptic object perception for robots: an overview," *Autonomous Robots*, vol. 47, no. 4, pp. 377–403, 2023.

[2] S. Luo, J. Bimbo, R. Dahiya, and H. Liu, "Robotic tactile perception of object properties: A review," *Mechatronics*, vol. 48, pp. 54–67, 2017.

[3] C. Du Toit, A. Chinsamy, and S. Cunningham, "Cretaceous origins of the vibrotactile bill-tip organ in birds," *Proceedings of the Royal Society B*, vol. 287, no. 1940, p. 20202322, 2020.

[4] P. Richard, M. Nicodemi, R. Delannay, P. Ribiere, and D. Bideau, "Slow relaxation and compaction of granular systems," *Nature materials*, vol. 4, no. 2, pp. 121–128, 2005.

[5] W. Swick and J. Perumpral, "A model for predicting soil-tool interaction," *Journal of Terramechanics*, vol. 25, no. 1, pp. 43–56, 1988.

[6] S. Jia, L. Zhang, and V. J. Santos, "Autonomous tactile localization and mapping of objects buried in granular materials," *IEEE Robotics and Automation Letters*, vol. 7, no. 4, pp. 9953–9960, 2022.

[7] S. Jia and V. J. Santos, "Tactile perception for teleoperated robotic exploration within granular media," *ACM Transactions on Human-Robot Interaction (THRI)*, vol. 10, no. 4, pp. 1–27, 2021.

[8] Z. Zhang, R. Jia, Y. Yan, R. Han, S. Lin, Q. Jiang, L. Zhang, and J. Pan, "Grains: Proximity sensing of objects in granular materials," *arXiv preprint arXiv:2307.05935*, 2023.

[9] R. Patel, R. Ouyang, B. Romero, and E. Adelson, "Digger finger: Gel-sight tactile sensor for object identification inside granular media," in *Experimental Robotics: The 17th International Symposium*, pp. 105–115, Springer, 2021.

[10] T. Syrymova, Y. Massalim, Y. Khassanov, and Z. Kappassov, "Vibro-tactile foreign body detection in granular objects based on squeeze-induced mechanical vibrations," in *2020 IEEE/ASME International Conference on Advanced Intelligent Mechatronics (AIM)*, pp. 175–180, IEEE, 2020.

[11] Z. Zhang, G. Zheng, X. Ji, G. Chen, R. Jia, W. Chen, G. Chen, L. Zhang, and J. Pan, "Mae4gm: Visuo-tactile learning for property estimation of granular material using multimodal autoencoder,"

[12] T. P. Tomo, A. Schmitz, W. K. Wong, H. Kristanto, S. Somlor, J. Hwang, L. Jamone, and S. Sugano, "Covering a robot fingertip with uskin: A soft electronic skin with distributed 3-axis force sensitive elements for robot hands," *IEEE Robotics and Automation Letters*, vol. 3, pp. 124–131, 2018.

[13] T. P. Tomo, M. Regoli, A. Schmitz, L. Natale, H. Kristanto, S. Somlor, L. Jamone, G. Metta, and S. Sugano, "A new silicone structure for uskin—a soft, distributed, digital 3-axis skin sensor and its integration on the humanoid robot icub," *IEEE Robotics and Automation Letters*, vol. 3, no. 3, pp. 2584–2591, 2018.

[14] A. A. Bonzini, L. Seminara, S. Macciò, A. Carfı, and L. Jamone, "Leveraging symmetry detection to speed up haptic object exploration in robots," in *2022 IEEE International Conference on Development and Learning (ICDL)*, pp. 95–100, IEEE, 2022.

[15] B. J. Kaus, "Factors that control the angle of shear bands in geodynamic numerical models of brittle deformation," *Tectonophysics*, vol. 484, no. 1-4, pp. 36–47, 2010.

[16] Q. Li, O. Kroemer, Z. Su, F. F. Veiga, M. Kaboli, and H. J. Ritter, "A review of tactile information: Perception and action through touch," *IEEE Transactions on Robotics*, vol. 36, no. 6, pp. 1619–1634, 2020.

[17] S. E. Navarro, M. Marufo, Y. Ding, S. Puls, D. Göger, B. Hein, and H. Wörn, "Methods for safe human-robot-interaction using capacitive tactile proximity sensors," in *2013 IEEE/RSJ International Conference on Intelligent Robots and Systems*, pp. 1149–1154, IEEE, 2013.

[18] L.-T. Jiang and J. R. Smith, "Seashell effect pretouch sensing for robotic grasping.," in *ICRA*, pp. 2851–2858, 2012.

[19] D. Guo, P. Lancaster, L.-T. Jiang, F. Sun, and J. R. Smith, "Transmissive optical pretouch sensing for robotic grasping," in *2015 IEEE/RSJ International Conference on Intelligent Robots and Systems (IROS)*, pp. 5891–5897, IEEE, 2015.

[20] T. Schlegl, M. Neumayer, S. Mühlbacher-Karrer, and H. Zangl, "A pretouch sensing system for a robot grasper using magnetic and capacitive sensors," *IEEE Transactions on Instrumentation and Measurement*, vol. 62, no. 5, pp. 1299–1307, 2013.

[21] A. C. Holgado, T. P. Tomo, S. Somlor, and S. Sugano, "A multimodal, adjustable sensitivity, digital 3-axis skin sensor module," *Sensors*, vol. 20, no. 11, p. 3128, 2020.

[22] R. Fagiani, F. Massi, E. Chatelet, Y. Berthier, and A. Akay, "Tactile perception by friction induced vibrations," *Tribology International*, vol. 44, no. 10, pp. 1100–1110, 2011.

[23] M. Sagara, L. Nobuyama, and K. Takemura, "Nonlinear tactile estimation model using vibration information from tactile sensor mediated by mechanoreceptors' perceptibility," in *2021 IEEE Sensors*, pp. 1–4, IEEE, 2021.

[24] D. M. Mueth, H. M. Jaeger, and S. R. Nagel, "Force distribution in a granular medium," *Physical Review E*, vol. 57, no. 3, p. 3164, 1998.

[25] J. Peters, M. Muthuswamy, J. Wibowo, and A. Tordesillas, "Characterization of force chains in granular material," *Physical Review E—Statistical, Nonlinear, and Soft Matter Physics*, vol. 72, no. 4, p. 041307, 2005.

[26] N. Brodu, J. A. Dijksman, and R. P. Behringer, "Spanning the scales of granular materials through microscopic force imaging," *Nature communications*, vol. 6, no. 1, p. 6361, 2015.